

High power burst-mode optical parametric amplifier with arbitrary pulse selection

M. Pergament,^{*} M. Kellert, K. Kruse, J. Wang, G. Palmer, L. Wissmann, U. Wegner
and M. J. Lederer

European X-Ray Free-Electron Laser-Facility GmbH, Albert-Einstein-Ring 19, 22761 Hamburg, Germany
^{*}mikhail.pergament@xfel.eu

Abstract: We present results from a unique burst-mode femtosecond non-collinear optical parametric amplifier (NOPA) under development for the optical - x-ray pump-probe experiments at the European X-Ray Free-Electron Laser Facility. The NOPA operates at a burst rate of 10Hz, a duty cycle of 2.5% and an intra-burst repetition rate of up to 4.5MHz, producing high fidelity 15fs pulses at a center wavelength of 810nm. Using dispersive amplification filtering of the super-continuum seed pulses allows for selectable pulse duration up to 75fs, combined with a tuning range in excess of 100nm whilst remaining nearly transform limited. At an intra-burst rate of 188kHz the single pulse energy from two sequential NOPA stages reached 180μJ, corresponding to an average power of 34W during the burst. Acousto- and electro-optic switching techniques enable the generation of transient free bursts of required length and the selection of arbitrary pulse sequences inside the burst.

© 2014 Optical Society of America

OCIS codes: (140.7090) Ultrafast lasers; (190.4970) Parametric oscillators and amplifiers; (190.4410) Nonlinear optics, parametric processes.

References and links

1. “Technical Design Report (TDR) of the European XFEL” (Chapter 4: XFEL Accelerator) http://XFEL.desy.de/local/Explorer_read?currentPath=/afs/desy.de/group/XFEL/woj/EPT/TDR/XFEL-TDR-Ch-4.pdf
2. A. Dubietis, G. Jonusauskas, and A. Piskarskas, “Powerful femtosecond pulse generation by chirped and stretched pulse parametric amplification in BBO crystal,” *Opt. Commun.* **88**(4-6), 437–440 (1992).
3. I. N. Ross, P. Matousek, M. Towrie, A. J. Langley, and J. L. Collier, “The prospects for ultrashort pulse duration and ultrahigh intensity using optical parametric chirped pulse amplifiers,” *Opt. Commun.* **144**(1-3), 125–133 (1997).
4. G. Cerullo and S. De Silvestri, “Ultrafast optical parametric amplifiers,” *Rev. Sci. Instrum.* **74**(1), 1 (2003).
5. R. Riedel, A. Stephanides, M. J. Prandolini, B. Gronloh, B. Jungbluth, T. Mans, and F. Tavella, “Power scaling of supercontinuum seeded megahertz-repetition rate optical parametric chirped pulse amplifiers,” *Opt. Lett.* **39**(6), 1422–1424 (2014).
6. J. Rothhardt, S. Demmler, S. Hädrich, J. Limpert, and A. Tünnermann, “Octave-spanning OPCPA system delivering CEP-stable few-cycle pulses and 22 W of average power at 1 MHz repetition rate,” *Opt. Express* **20**(10), 10870–10878 (2012).
7. M. J. Lederer, M. Pergament, M. Kellert, and C. Mendez, “Pump-probe laser development for the European X-Ray Free-Electron Laser Facility,” Paper 8504-20, SPIE Conference on Optics and Photonics 2012, 12–16 August 2012, San Diego, invited talk.
8. K. Kruse, M. Pergament, M. Kellert, C. Mendez, G. Kulcsar, and M. J. Lederer, “All-fiber 1030nm burst-mode front-end amplifier for the European XFEL pump-probe laser development for the European X-Ray Free-Electron Laser Facility,” Paper Mo4.5, Ultrafast Optics Conference IX, 04–08 March 2013, Davos.
9. P. Russbuehler, T. Mans, G. Rotarius, J. Weitenberg, H. D. Hoffmann, and R. Poprawe, “400W Yb:YAG Innoslab fs-Amplifier,” *Opt. Express* **17**(15), 12230–12245 (2009).
10. M. Kellert, K. Kruse, M. Pergament, G. Kulcsar, T. Mans, and M. J. Lederer, “High power femtosecond 1030nm burst-mode front-end and pre-amplifier for the European XFEL pump-probe laser development,” Poster CA-P.23, Conference on Lasers and Electro-Optics (CLEO) 2013, 12–16 May 2013, Munich.
11. M. Emons, A. Steinmann, T. Binhammer, G. Palmer, M. Schultze, and U. Morgner, “Sub-10-fs pulses from a MHz-NOPA with pulse energies of 0.4 μJ,” *Opt. Express* **18**(2), 1191–1196 (2010).

12. M. Bradler, P. Baum, and E. Riedle, "Femtosecond continuum generation in bulk laser host materials with sub- μ J pump pulses," *Appl. Phys. B* **97**(3), 561–574 (2009).
 13. J. Bromage, J. Rothhardt, S. Hädrich, C. Dorrer, C. Joher, S. Demmler, J. Limpert, A. Tünnermann, and J. D. Zuegel, "Analysis and suppression of parasitic processes in noncollinear optical parametric amplifiers," *Opt. Express* **19**(18), 16797–16808 (2011).
 14. D. N. Nikogosyan, "Beta Barium Borate (BBO) a review of its properties and applications," *Appl. Phys., A Mater. Sci. Process.* **52**(6), 359–368 (1991).
 15. D. N. Nikogosyan, "Lithium Triborate (LBO) a review of its properties and applications," *Appl. Phys., A Mater. Sci. Process.* **58**(3), 181–190 (1994).
 16. J. Moses, C. Manzoni, S.-W. Huang, G. Cerullo, and F. X. Kärtner, "Temporal optimization of ultrabroadband high-energy OPCPA," *Opt. Express* **17**(7), 5540–5555 (2009).
-

1. Introduction

The European X-ray Free Electron Laser Facility (European XFEL) is currently under construction, aiming at unprecedented time-averaged X-ray power density [1]. In operation, it will generate up to 27000 x-ray femtosecond pulses per second. It is designed to deliver such a high number of pulses in burst-mode at a burst rate of 10Hz. Each burst is 600 μ s in duration, containing up to 2700 pulses, which corresponds to an intra-burst repetition rate of 4.5MHz. The target pulse duration of the European XFEL lies in the range of sub-10fs to 100fs, driven by experimental requirements in diverse scientific fields such as biology, material science, nanophysics and chemistry. A significant amount of the experiments (up to 75%) will require an optical laser for pump-probe experiments. Naturally, a pump-probe (PP) laser for the European XFEL must be adapted to its lasing-mode, i. e. it should deliver synchronized pulses of comparable pulse width within 10Hz bursts of 600 μ s length and an intra-burst repetition rate up to 4.5MHz. Some degree of freedom in the choice of pulse width and wavelength (around 800nm) is also desirable. Energy requirements for single pulses usually range from μ J to mJ. Moreover, different experiments need different repetition rates and pulse patterns inside the burst and a quick change of repetition rate often helps in determining the influence of thermal load on the sample. In consideration of such difficult demands, it is clear that no single commercial laser technology is currently capable of fulfilling them. Nevertheless, there are two principle technologies that can be considered for the design of such a laser source. Firstly, the use of Ti:sapphire based oscillator and amplifier combinations and, secondly, optical parametric amplification (OPA) of a broadband seed source. Although these approaches are fundamentally different, they both require very similar pulsed pump sources in the green for synchronous pumping of the amplifiers. However, amongst other reasons, considering the high single pass amplification of an OPA and in particular the superior short pulse capability of non-collinear OPAs (NOPAs) [2–6], this technology appears more suitable for the task. Therefore, we have proposed a multi-stage NOPA concept, employing an Yb-based synchronized front-end, Yb:YAG Innoslab pump amplifiers and dispersion managed super-continuum seed [7–10]. In this paper we present the current status of the European XFEL PP-laser development. With the exception of further scaling of pulse energy and average power, all essential features were achieved:

- essentially pedestal-free 15fs pulses at an intra-burst repetition rate of up to 4.5MHz and center wavelength of 810nm.
- pulse energy of 180 μ J from two sequential NOPA stages with an intra-burst repetition rate of 188kHz.
- possibility of generating longer pulses (up to 75fs), enabling efficient non-linear conversion as well as wavelength tuning over a range of more than 100 nm.
- diffraction-limited beam quality.
- transient free bursts and arbitrary pulse selection from single pulses to 4.5MHz.

2. Experimental setup

Figure 1 shows a schematic of the PP-laser system for which current results are reported. A low-jitter 54MHz, 1030nm femtosecond oscillator, which will finally be synchronized to the European XFEL, provides 170fs seed pulses to an all-fiber chirped pulse front-end amplifier with two inherently synchronized outputs, XF 1 and XF 2 [8, 10]. The 1ns long chirped pulses from XF 1 seed an Innoslab Yb:YAG [9, 10] power amplifier, bringing it to full output power, independent of the intra-burst repetition rate. In this mode, a change of repetition rate entails a corresponding change in pulse energy. All amplifiers are pumped in burst-mode at 10Hz with burst lengths of a few milliseconds, raising the power level to 400W during that time only. To achieve the necessary beam quality for second harmonic generation and NOPA pumping, some low level side-lobes needed to be filtered from the pump beam at a loss of less than 5%. A Pockels-cell (PC) was inserted before the compressor. It enables the picking of arbitrary pulse sequences from the amplified burst up to a repetition rate of 4.5MHz (see section 3.5). Two NOPA configurations were tested, corresponding to the intra-burst repetition rate settings of 4.5MHz (NOPA I only) and 188kHz (NOPA I + NOPA II). After compression in a multi-layer dielectric grating compressor, the infrared pump pulse duration is 800fs and pulse energies are 77 μ J at 4.5 MHz and 1.9mJ at 188 kHz. In the latter case the pump pulse is split into two replicas to pump NOPA I at the same intensity as in the case of 4.5MHz. Conversion to the green is achieved with an efficiency of about 65%, resulting in pump energies of 45 μ J for NOPA I and 1.19 mJ for NOPA II. From the measured pump beam sizes (Fig. 2), peak intensities on the surface of the NOPA crystals were calculated to be 34 GW/cm² (NOPA I) and 37GW/cm² (NOPA II).

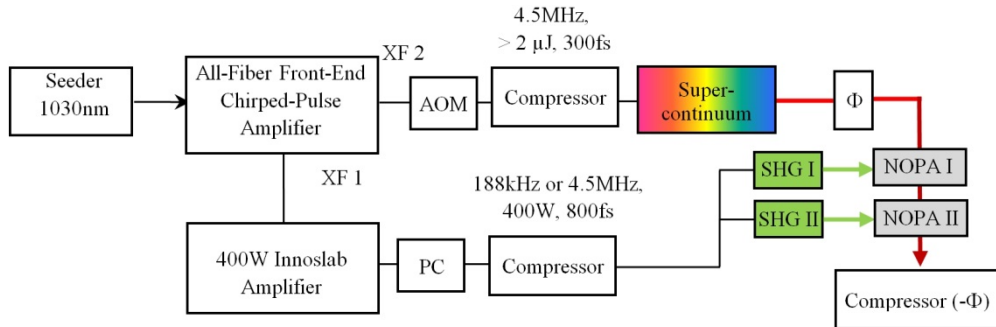


Fig. 1. Schematic of PP-laser prototype; AOM (Acousto-Optical Modulator), PC (Pockels Cell), SHG (Second Harmonic Generation), Φ multi-bounce chirped mirror stretcher, NOPA (Non-collinear Optical Parametric Amplifier), $-\Phi$ fused silica compressor.

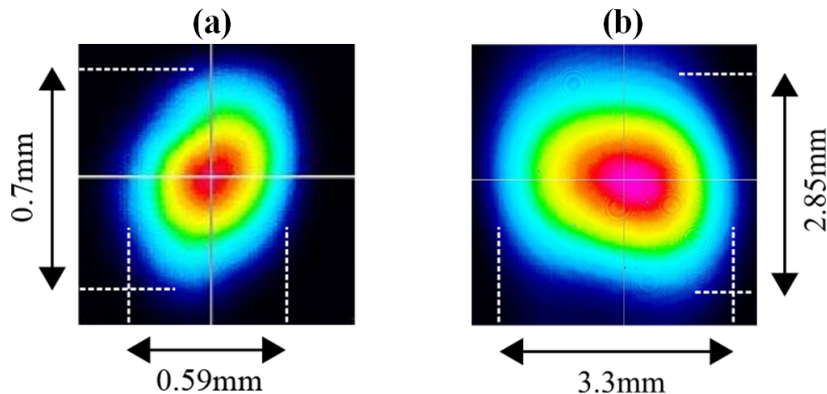


Fig. 2. Near field profiles of the pump beams (515nm) on the NOPA crystal surfaces. (a) NOPA I; (b) NOPA II ($1/e^2$, from Gaussian fit).

The second output (XF2) of the front-end amplifier is used to generate white light supercontinuum (WLC) to seed the NOPA [11, 12]. Before compression to a pulse width of 300fs, an acousto-optic modulator (AOM) was inserted for pulse selection (see section 3.4). The intra-burst frequency of XF 2 is fixed at 4.5MHz, from which all lower frequencies in XF 1 are also derived. WLC has proven to be a stable and reliable seed source for ultra-short pulse parametric amplifiers, assuring excellent beam quality and compressibility. Two crystals, namely YAG and KGW, were tested for that purpose, motivated by their high values of nonlinear refractive index [12].

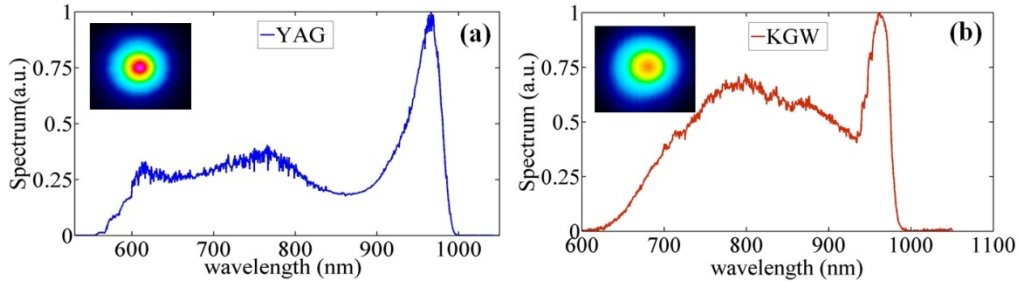


Fig. 3. Spectral and beam characteristics of WLC in the spectral region of interest. (a) Spectrum from 5mm YAG, $E = 7.2$ nJ; (b) spectrum from 6mm KGW, $E = 4.6$ nJ. The insets show the corresponding near-field beam profiles.

For that purpose, XF 2 pulses were focused into the crystals with an NA of 0.02, reaching long term stable continuum generation at pulse energies of $0.725\mu\text{J}$ and $0.280\mu\text{J}$ in YAG and KGW respectively, comparable to previously published values [12]. Figure 3 shows the spectral and beam characteristics in the spectral region of interest. Due to the higher energy content in the case of YAG (7.2nJ) compared to KGW (4.6nJ), the former was chosen for our setup. In the following sections we will use the term “signal” when referring to the continuum seed.

3. Results

3.1 Short pulse mode BBO-NOPA

Before amplification, the signal pulses are negatively chirped by multiple bounces off a compensated pair of chirped mirrors (Φ , see Fig. 1), whose combined dispersion curve is conjugate to that of bulk fused silica, which is used for compression ($-\Phi$, see Fig. 1). With one bounce corresponding to 2mm of fused silica and a total of 32 bounces, the seed pulses are sufficiently stretched (to about 800fs) for the NOPA pump pulses to sample and amplify the maximum amount of seed spectrum, which is still well controlled by the chirped mirrors (roughly from 720nm to 900nm). The energy working point of NOPA I was the same for both configurations (4.5MHz, NOPA I and 188kHz, NOPA I + NOPA II). The different average powers in these cases do not cause any discernable difference in the amplification. NOPA I is a 2.2 mm thick Beta-Barium Borate (BBO) crystal (type- I, 24.6° phase matching angle) with an internal non-collinearity of $\alpha = 2.6^\circ$, which corresponds to the magic angle for broadband amplification. The seed beam diameter is only slightly smaller than that of the pump beam (Fig. 2) in order to optimize efficiency. The signal pulse energy after amplification is $5\mu\text{J}$, leading to an output to pump pulse efficiency of 11% and a gain of more than 1000. The output spectrum is close to 160nm (full width at -10dB level), capable of supporting pulses shorter than 15fs. In case of 2-stage operation at 188 kHz the output of the first stage is re-imaged to the second stage with a magnification of approximately 6 in order to match the size of the pump beam (Fig. 2).

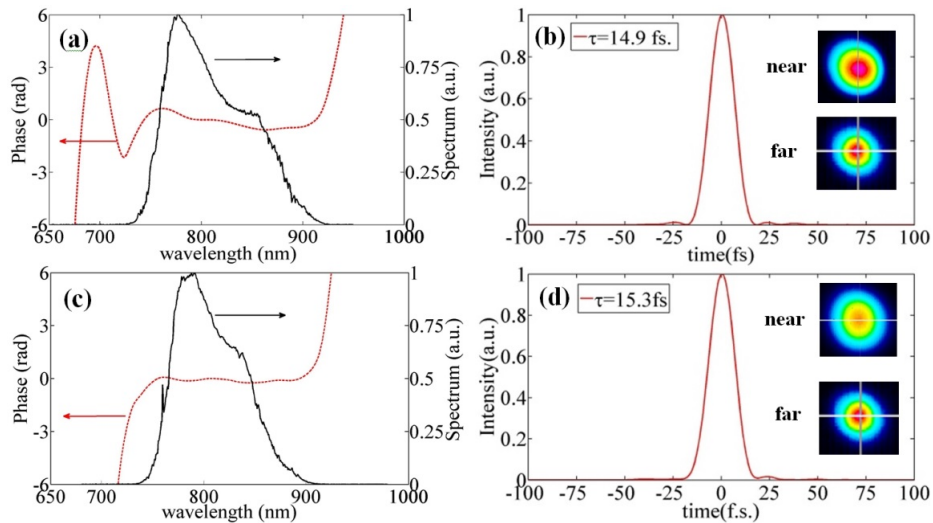


Fig. 4. Characterization of amplified pulses for NOPA I + NOPA II at 188kHz. (a) BBO-NOPA output spectrum (black), spectral phase (red, dotted) and (b) reconstructed temporal pulse shape. (c) LBO-NOPA output power spectrum (black), spectral phase (red, dotted) and (d) reconstructed temporal pulse shape. The insets depict near and far field beam profiles.

NOPA II consists of a 1.5mm thick BBO crystal of the same cut. The re-imaged output of the first stage is overlapped with the pump beam at the same internal non-collinearity as in NOPA I. The resultant pulse energy after amplification is $180\mu\text{J}$, leading to an overall output to pump pulse efficiency of 15%. At 188 kHz this yields an average power of 34W during the burst. After amplification, the pulses were compressed by 42mm of fused silica. Figure 4 shows the spectrum and spectral phase [Fig. 4(a)] and the reconstructed pulse 4(b) using spectral phase interferometry for direct electric field reconstruction (SPIDER). The spectra were also cross-checked using an optical spectrum analyzer (ANDO AQ6315-A). The reconstructed pulse duration equals 14.9 fs (FWHM), with a peak to pedestal contrast of around 100. The spectrum reveals a width of nearly 155nm (full width at -10dB) and supports pulses with a theoretical Fourier limited duration of 13.8fs. We attribute the slight discrepancy to uncompensated higher order dispersion contributions. From a measurement of the beam shape in the far and near field [insets in Fig. 4(b)], we estimate an $M^2 < 1.15$. Finally, we note that both NOPA crystals were oriented in the so called non-walk-off compensation direction, avoiding phase-matched parasitic frequency mixing processes [13].

3.2 Short pulse mode LBO-NOPA

One of the problems of parametric amplification in high average power laser systems is the absorption of the pump in the nonlinear crystals. The rise of crystal temperature due to absorption could lead to changes in the indicatrix and hence a change of phase matching conditions which, in turn, can decrease the amplification efficiency. One possible solution is to employ crystals with lower absorption at the pump wavelength. The most obvious candidate for that is Lithium Triborate (LBO), which can be manufactured with significantly smaller absorption than BBO [14, 15] whilst promising comparable NOPA performance. For that reason we tested a two-stage LBO amplifier under the same conditions (pump, seed, and dispersion management), with crystal lengths scaled according to the lower nonlinear coefficient of LBO. The signal is amplified in the first stage (4mm thick LBO, type-I, 16.5° phase matching angle, 1.6° internal non-collinearity) and re-imaged to the second, 3mm thick, LBO. The resultant signal energy of $175\mu\text{J}$ from the second stage is close to the result we have reached with the BBO amplifier. Following the amplification, the pulses are compressible by approximately the same thickness of fused silica. The spectral width of

127nm (full width at -10dB) [Fig. 4(c)] supports a Fourier limited pulse duration of 14.7fs, compared with the reconstructed pulse duration of 15.3fs [Fig. 4 (d)]. An estimation of the beam quality was again determined from near and far field measurements, resulting in $M^2 < 1.13$ [insets in Fig. 4(d)]. Although we do not observe any detrimental effects from pump-absorption in BBO at the current power levels, we consider the essentially equivalent performance (spectral, temporal, gain, etc.) of our LBO-NOPA very encouraging for future power scaling.

3.3 Long pulse mode BBO-NOPA

For different reasons, facility users inquire about the possibility of longer pulses and wavelength tuning of the PP-laser, whilst maintaining nearly transform limited pulses. Our approach towards longer, nearly transform limited pulses is to simply stretch the signal stronger in order to amplify a narrower portion of the spectrum, temporally overlapped with pump pulse [16]. However, the previously used dispersion management scheme would require an excessive number of reflections on the chirped mirrors and a correspondingly long block of fused silica for compression, making the setup rather impractical. Hence, a new scheme for dispersion management was implemented, where the signal is chirped positively by bulk fused silica before amplification and additionally subjected to multiple bounces off a pair of chirped mirrors. These are designed such that for suitable combinations of material length and number of bounces, the total dispersion before amplification is conjugate to that of a Treacy compressor.

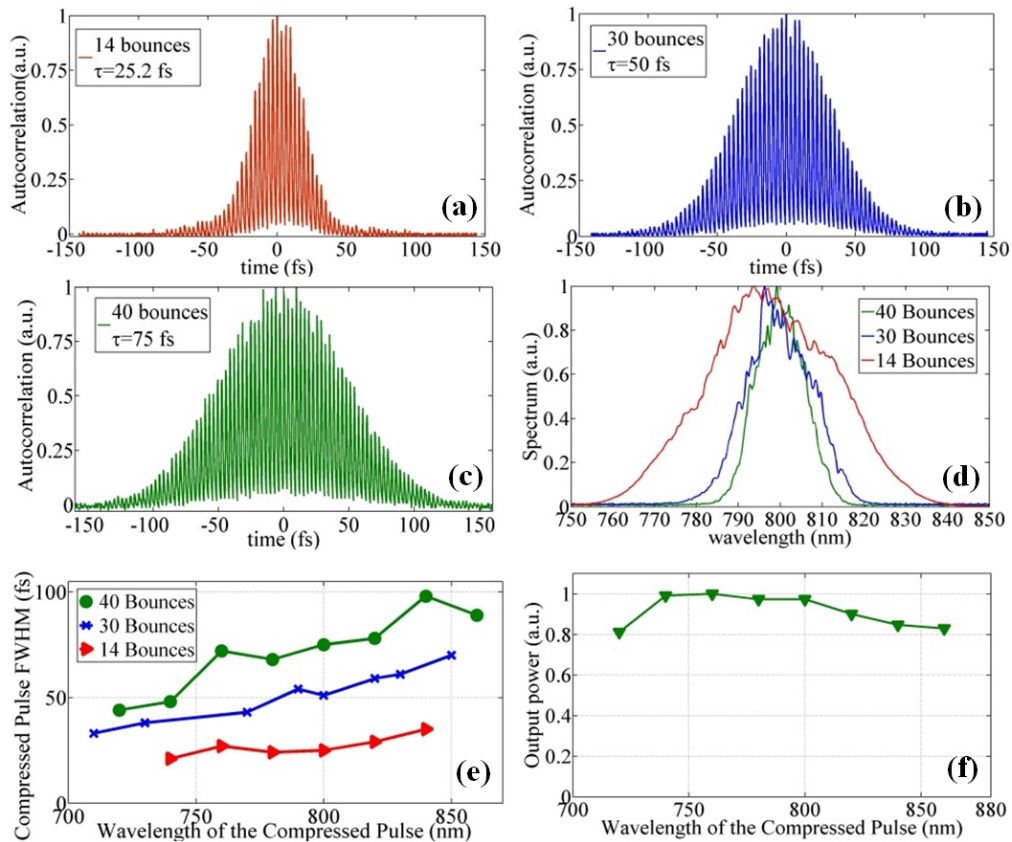


Fig. 5. Characterization of amplified pulses after compression in long pulse mode BBO-NOPA. Intensity autocorrelation with (a) 14 bounces; (b) 30 bounces and (c) 40 bounces; (d) corresponding spectra; (e) tuning curves; (f) power variation upon tuning (40 bounces).

The latter was built from 1250 lines/mm transmission gratings and had an efficiency of 80%. The two-stage BBO NOPA was operating under the same pump and crystal conditions as discussed in section 3.1.

Three different dispersion settings were tested, resulting in compressed pulses of 25fs, 50fs and 75fs. Figures 5(a), 5(b) and 5(c) show the corresponding intensity autocorrelations from which the pulse widths were estimated assuming a sech^2 pulse shape. The corresponding spectra of all three settings are depicted in [Fig. 5(d)]. The compressed pulses are close to the transform limit, considering the spectra. After the compressor the pulse energy was measured to be 140 μ J and the beam quality was equal to that shown previously. With the flexibility of the transmission grating compressor, we believe it possible to create even longer pulses. Disregarding a slight dispersion mismatch in the higher orders, adding highly dispersive bulk material in the seed path should enable pulses in excess of 100fs, finally limited by the degrading energy density of the seed.

As additional feature, resulting from the reduced bandwidth of the longer pulses, it is possible to tune their center wavelength by changing the temporal delay of the seed relative to the fixed pump pulse. Figure 5(e) shows the tuning curves achieved that way. Accepting a certain variation in pulse width, the tuning range corresponds to 100nm or larger in all cases. We attribute the variation in pulse width over the tuning range mainly to a deviation of the chirped mirror dispersion from the ideal design. The output power variation due to wavelength tuning is in the range of 20% [Fig. 5(f)].

3.4 Pulse and burst stability

For a burst-mode laser, an important stability criterion concerns the fluctuation of the total burst energy. For the setup in our lab, we determined an rms value of 1.5%. We believe it could be improved somewhat through more careful considerations of air currents. Another concern is the intra-burst pulse to pulse stability of various parameters. Unfortunately, a direct measurement of pulse to pulse characteristics within the same burst, such as beam shape, spectrum and compression, is problematic at high repetition rates. This relates to exposure time and repetition rate limits of standard analysis devices. As for the pulse energy distribution across a burst, we used a photodiode and an 8GHz oscilloscope with high sampling rate and statistical tools to extract energy statistics. Both using an integrating sphere, or simply under-filling the photodiode, resulted in an rms value of 1% during a 600 μ s long section of interest. Figure 6(a) depicts the complete burst as it is amplified by the NOPA. The burst length of 2.5ms is determined by the length of the pump burst. A slight transient is observed during the first millisecond, after which a 600 μ s long section can be selected. Given both stability measurements, we conclude that a burst-to-burst scanning approach is justifiable for measurements of the spectral and beam shape evolution during the burst.

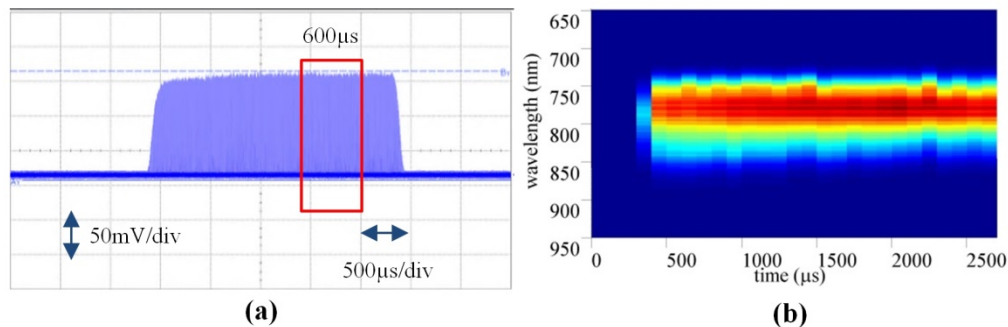


Fig. 6. Characteristics of the burst. (a) Burst output from the NOPA observed with a fast photodiode; (b) intra-burst spectral scan.

The spectral scan was made with an STS-IR Ocean Optics spectrometer with relative irradiance calibration from 600nm to 1100nm. The exposure time was 10 μ s, capturing at most two pulses per burst at 188 kHz. The scan was performed with a step size of 100 μ s. Figure 6(b) shows the spectral evolution during the burst, taken over a scanning time of 15 minutes and without active pump-seed arrival time stabilization. The same type of measurement was performed to investigate the evolution of the near-field profile. The CCD camera featured an exposure time of 40 μ s, integrating over seven pulses at 188 kHz. Again the scan was done with 100 μ s step resolution. The result of the scan is presented in (Fig. 7). It reveals a stable beam shape following a transient phase of around 1ms.

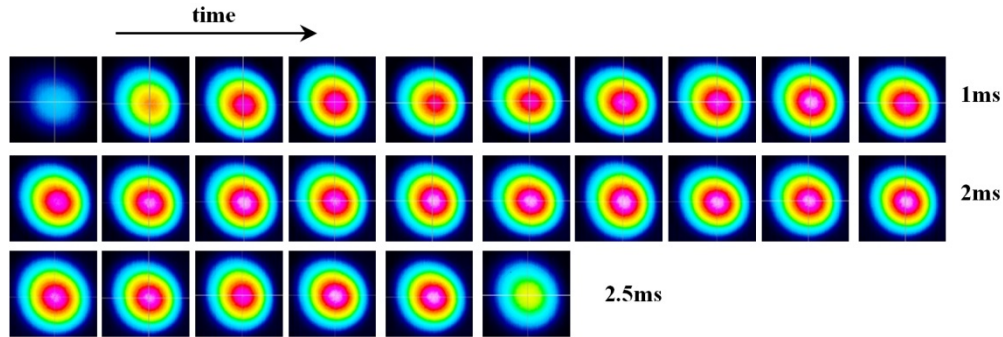


Fig. 7. Intra-burst near-field profile scan (100 μ s steps).

3.5 Burst shaping and arbitrary pulse selection

The linear accelerator of the European XFEL provides a 600 μ s long electron bunch train, resulting in an equivalent x-ray burst in case all electrons were to pass through a single undulator. In most cases however, the bunch train is sliced in two parts, supplying electrons to different undulators. Moreover, undulators can be prevented from lasing on a bunch-to-bunch case, resulting in the possibility of arbitrary pulse patterns. Therefore, it is important for the PP-laser to provide a similar feature for flexibility of choosing different burst length and arbitrary pulse sequences on demand and without major interference with the laser working point. There are two equivalent ways to pick pulses in the parametric amplifier. The first way is to pick the signal pulses to be amplified in the NOPA. Since at the chosen pump intensity amplified super-fluorescence is negligible, there is no output in the absence of a seed pulse. The second way is to pick the pump pulses. With a seed pulse energy of a few nJ, the output is also negligible in this case.

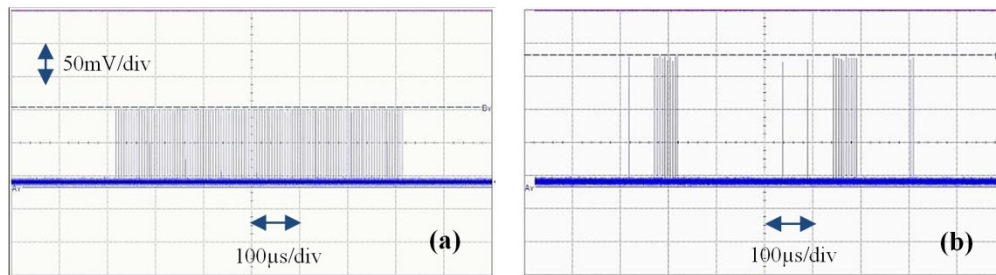


Fig. 8. “Pulse on demand” using the AOM. NOPA I + NOPA II produce 180 μ J pulses at 15fs.
(a) Cut-out 600 μ s burst, (b) arbitrarily picked pattern of pulses.

Both methods were implemented successfully in the system. The seed pulse selection was realized with an AOM installed after the XF2 output (Fig. 1, AOM). The AOM was working in the zeroth order, simply decreasing transmission by about 50% for those pulses that were to

be suppressed. This prevents the generation of super-continuum entirely, resulting in a lack of signal. The AOM can be activated at a rate in excess of 4.5MHz. Picking of the pump pulses was performed by a large aperture BBO Pockels cell placed behind the 400W amplifier (Fig. 1, PC). Also here, the driver has the capability of switching the PC in half-wave configuration at a rate up to 4.5MHz. Figure 8 shows examples for the shaping of a clean and transient free burst and the picking of arbitrary pulse sequences using the AOM (“pulse-on-demand”). It was verified that both methods are indeed equivalent. The use of the PC is particularly interesting for cases where the NOPA pump laser might be used as an independent source in experiments. We verified that the pulse parameters under picking conditions are equivalent to those without picking by performing spectral and SPIDER measurements of single pulses picked from the burst. From this we conclude that all involved processes (super-continuum generation and parametric amplification) are in effect instantaneous at the power levels currently employed.

4. Summary

The concept of the burst-mode pump-probe laser for the European XFEL was presented together with first experimental results. Apart from the basic requirements of 10Hz burst-mode operation with intra-burst frequencies up to 4.5MHz, we showed that the NOPA approach offers the flexibility to achieve also other useful features. From two sequential NOPA stages, we extracted essentially pedestal free 15fs pulses with 180 μ J pulse energy at a center wavelength of 810nm and with diffraction limited beam quality. Using dispersion management of the seed signal in combination with amplification filtering, we generated close to transform limited longer pulses (up to 75fs), combined with the possibility of wavelength tuning over a range of 100nm. The laser output is characterized by burst to burst and pulse to pulse energy fluctuations of <1.5% rms. Transient free arbitrary pulse selection and burst duration shaping were demonstrated. From the current results, we do not anticipate principle problems to scale the NOPA output energy and power further. An upgrade of pump power is under way.